The Statistical Model of Hadrogenesis in A–A collisions from AGS to SPS and RHIC*)

Krzysztof Redlich[a,+)]
[a] Theoretical Physics Division, CERN, CH-1211 Geneva 23, Switzerland

ABSTRACT

We discuss experimental data on particle yields and particle spectra obtained in heavy ion collisions in a very broad energy range from SIS/GSI ($\sqrt{s} \simeq 2$ GeV) through AGS/BNL ($\sqrt{s} \simeq 5$ GeV) up to SPS/CERN ($\sqrt{s} \simeq 20$ GeV) and RHIC/BNL ($\sqrt{s} \simeq 130$) GeV. We argue that in this broad energy range hadronic yields and their ratios resemble a thermal equilibrium population along a unified freeze–out curve determined by the condition of fixed energy/particle $\simeq 1$ GeV. At RHIC and top SPS, thermal parameters are consistent within error with the critical conditions required for deconfinement. This, together with the particular distribution of strangeness within a collision fireball, could indicate that chemical equilibrium is a direct consequence of parton to hadron transition, which populates a state of maximum entropy. At lower energies equilibration in A–A collisions should appear through hadronic interactions and rescatterings.

+) Permanent address: Institute of Theoretical Physics, University of Wrocław, PL-50204 Wrocław, Poland: redlich@rose.ift.uni.wroc.pl

*) Plenary talk given at: International Nuclear Physics Conference, INPC2001, Berkeley, USA, August 2001.

CERN-TH/2001-342
December 2001

1 Introduction

The ultimate goal of ultrarelativistic nucleus–nucleus collisions is to study the properties of strongly interacting matter under extreme conditions of high energy density [1]. Quantum Chromodynamics (QCD) predicts that strongly interacting matter undergoes a phase transition from a state of hadronic constituents to a plasma of unbounded quarks and gluons (QGP) [2, 3]. By colliding heavy ions at ultrarelativistic energies, one expects to create hadronic matter under that conditions are sufficient for deconfinement [1, 4, 5, 6, 7]. Thus, of particular relevance was finding experimental probes to check if the produced medium in its early stage was indeed in the QGP phase. Different probes have been theoretically proposed and studied in terms of SPS/CERN and most recently RHIC/BNL experiments. The most promising signals of QGP were related with particular properties of photons [8, 9], dileptons [8, 10] and hadron spectra [5, 6, 11]. The photon rate was expected to be enhanced if the QGP were formed in the initial state. The invariant mass distribution of dileptons should be modified by in-medium effects related with chiral symmetry restoration [10, 12]. The suppression of charmonium production was argued to be a consequence of the collective effects in a deconfined medium [1, 13].

Hadron multiplicities and their correlations are observables which can provide information on the nature, composition, and size of the medium from which they are originating. Of particular interest is the extent to which the measured particle yields are showing equilibration. The appearance of the QGP, that is a partonic medium being at (or close to) local thermal equilibrium, and its subsequent hadronization during phase transition should in general drive hadronic constituents towards chemical equilibrium [4, 5, 6, 14]. Consequently, a high level of chemical saturation, particularly for strange particles [15], could be related with the deconfined phase created at the early stage of heavy ion collisions.

The level of equilibrium of secondaries in heavy ion collisions was tested by analysing the particle abundances [5, 6, 16, 17, 18, 19] or their momentum spectra [11, 20, 21]. In the first case one establishes the chemical composition of the system, while in the second case additional information on dynamical evolution and collective flow can be extracted.

In this article we will discuss and analyse the experimental data on hadronic abundances obtained in ultrarelativistic heavy ion collisions, in a very broad energy range starting from RHIC/BNL ($\sqrt{s}$ = 130 A GeV), SPS/CERN ($\sqrt{s} \simeq$ 20 A GeV) up to AGS/BNL ($\sqrt{s} \simeq$ 5 A GeV) and SIS/GSI ($\sqrt{s} \simeq$ 2 A GeV) to test equilibration. We argue that the statistical approach provides a very satisfactory description of experimental data covering a wide energy range from SIS up to RHIC. We discuss the unified description of particle chemical freeze–out and the excitation function of different particle species. Introducing, in addition to thermal, also the transverse collective motion, the systematics of thermal freeze–out is also presented.

2 Initial conditions in A–A collisions and deconfinement

In ultrarelativistic heavy ion collisions, the knowledge of the critical energy density ϵ_c required for deconfinement is of particular importance as well as the equation of state (EoS) of strongly interacting matter. The value of ϵ_c is needed to establish the necessary initial conditions in heavy ion collisions to possibly create the QGP, whereas EoS is required as an input to describe

the space-time evolution of the collision fireball.

Both of these these pieces of information can be obtained today from first principal calculations by formulating QCD on the lattice and performing numerical Monte-Carlo simulations. In Fig. 1 we show the most recent results of lattice gauge theory (LGT) for energy density and pressure [23]. These results have been obtained in LGT for different numbers of dynamical fermions. The energy density is seen in Fig. 1 to exhibit a typical behaviour in a system with a phase transition: an abrupt change in the very narrow temperature range.[1] The corresponding pressure shows a smooth change with temperature. In the region below T_c the basic constituents of QCD, quarks and gluons, are confined within their hadrons and here the EoS is well parametrized by the hadron resonance gas. Above T_c the system appears in the QGP phase where quarks and gluons can penetrate distances that substantially exceed a typical size of hadrons. The most recent results of improved perturbative expansion of thermodynamical potential in the continuum QCD [24] are showing that at some distance above T_c the EoS of QGP can be well described by a gas of massive quasi-particles whose mass is temperature dependent. In the near vicinity of T_c the relevant degrees of freedom were argued to be described by the Polyakov loops [25].

Lattice Gauge Theory predicts that in two–flavour QCD the critical temperature $T_c = 173 \pm 8$MeV and the corresponding critical energy density $\epsilon_c = 0.6 \pm 0.3$ GeV/fm^3 are required for chiral phase transition [23]. The value of ϵ_c is relatively low and quantitatively corresponds to the energy density inside the nucleon.

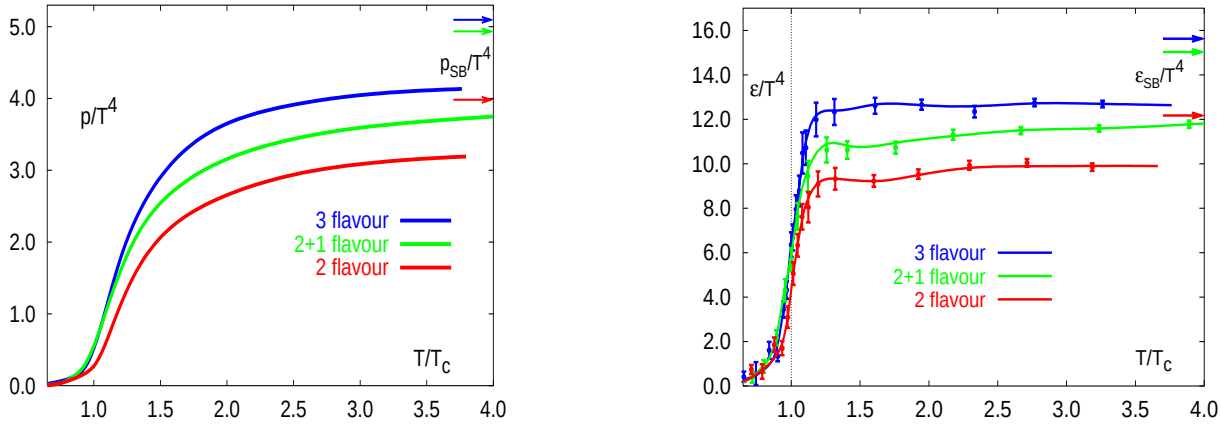

Figure 1: Pressure P and energy density normalized to temperature in fourth power, versus temperature normalized to its critical value. The calculations were done within LGT for different numbers of flavours [23]. The values of the corresponding ideal gas results are indicated by arrows.

The initial energy density reached in heavy ion collisions can be estimated within the Bjorken model [26]. From the rapidity distribution of protons and their transverse energy E_T measured in nucleus–nucleus collisions the initial energy density ϵ_0 is determined from

[1] We have to point out, however, that in the strictly statistical physics sense, a phase transition can only appear in the limit of massless quarks.

$$\epsilon_0(\tau_0) = \frac{1}{\pi R^2}\frac{1}{\tau_0}\frac{dE_T}{dy}. \quad (1)$$

where the initially produced collision fireball is considered as a cylinder of length $\tau_0 dy$ and transverse size $R \sim A^{1/3}$. Inserting for πR^2 the overlap area of colliding Pb nuclei together with initial time an $\tau_0 \simeq 1$ fm, and using an average transverse energy at midrapidity measured at the SPS ($\sqrt{s} = 17.3$ GeV) to be 400 GeV [27], one obtains

$$\epsilon_0^{SPS}(\tau_0 \simeq 1 \text{ fm}) \simeq 3.5 \pm 0.5 \text{ GeV/fm}^3. \quad (2)$$

Increasing the collision energy to $\sqrt{s} = 130$ A GeV for Au–Au at RHIC and keeping the same initial thermalization time as at the SPS, one would expect an increase of ϵ_0 by only 50–60 %. However, at RHIC the thermalization is argued, within saturation models, to appear at much shorter time. The basic concept of saturation models is a conjecture that there is some transverse momentum scale $p_{\rm sat}$ where the gluon and quark phase space density saturates [28]. For isentropic expansion of the collision fireball, one can relate the transverse energy at $p_{\rm sat}$ with the one measured in nucleus–nucleus collisions in the final state. The saturation scale also fixes the time scale $\tau_0 = 1/p_{\rm sat}$. Taking the value of $p_{\rm sat}$ predicted in [29] for RHIC $p_{\rm sat} \simeq 1.13$ GeV, one gets $\tau_0 \simeq 0.2$ fm and the corresponding initial energy density $\epsilon_0 \simeq 98$ GeV/fm^3. The estimate of ϵ_0, however, strongly depends on the value of $p_{\rm sat}$, which is model–dependent. The McLerran–Vanugopalan model [30], for instance, predicts the value of $\epsilon_0^{RHIC} \sim 20$ GeV/fm^3, which agrees with the predictions of [31]. At the SPS the saturation model described in [29] leads to $\epsilon_0^{SPS} \sim 16$ GeV/fm^3, a much higher value than given in Eq. (2). It is thus clear that there are large uncertainties on the value of the initial energy density reached in ultrarelativistic heavy ion collisions. In Pb–Pb collisions at the SPS according to the models one gets 2.5 GeV/fm^3 $< \epsilon_0^{SPS} <$ 16 GeV/fm^3 whereas in Au–Au collisions at RHIC, 20 GeV/fm^3 $< \epsilon_0^{SPS} <$ 100 GeV/fm^3.

The dominant component of the partonic medium produced in ultrarelativistic heavy ion collisions at RHIC and even at the SPS is gluons. The energy density of gluons in thermal equilibrium scales with the fourth power of the temperature $\epsilon = gT^4$, where g denotes the number of degrees of freedom. For an ideal gas, $g = 16\pi^2/30$; in an interacting system, the effective number of degrees of freedom g is smaller. The results of LGT shown in Fig. 1 indicate deviations from the Boltzmann limit by 20–25 %. Relating the thermal energy density with the initial energy density discussed above, one can make an estimate of the initial temperature reached in heavy ion collisions. For the SPS this gives a temperature in the range 200 MeV $< T <$ 330 MeV and at RHIC 400 MeV $< T <$ 600 MeV.

Comparing the initial energy density expected in heavy ion collisions with LGT results, it is clear that the initial energy density, at RHIC, exceeds by far the critical value. Thus, the necessary conditions to create the partonic medium in a deconfined phase are reached at RHIC as well as at the top SPS. Large energy density is, however, still not sufficient to create a QGP. The distribution of initially produced gluons is very far from being thermal, thus the system needs enough time to equilibrate. Recently, it was rigorously shown [32] in the framework of perturbative QCD and kinetic theory that the equilibration of partons happens indeed at the LHC and most likely at RHIC. Previous microscopic study within the Parton Cascade Model has also suggested that thermalization can be reached at lower SPS energy [33]. Here, however,

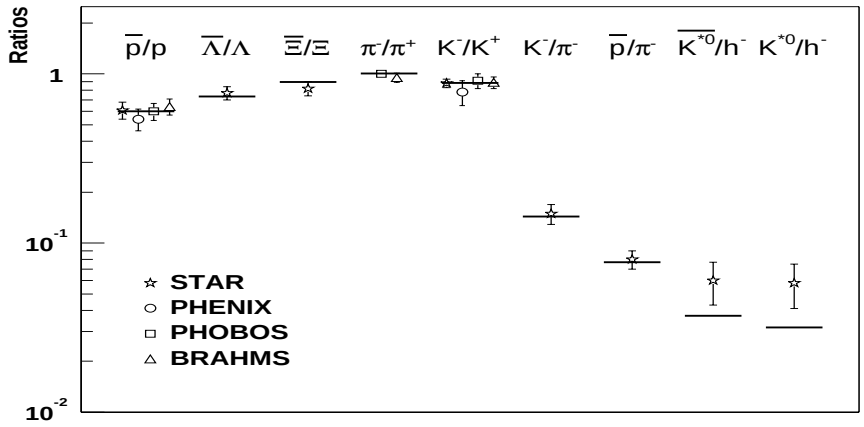

Figure 2: Comparison of the experimental data on different particle multiplicity ratios obtained at RHIC at ($\sqrt{s} = 130$) GeV with thermal model calculations for $T = 175$ MeV and $\mu_B = 51$ MeV.

it is not clear if models inspired by the perturbative QCD are indeed applicable at this relatively low collision energy.

Admitting QGP formation in the initial state in heavy ion collisions one could expect that the thermal nature of the partonic medium could be preserved during hadronization. Consequently, the particle yields measured in the final state should resemble the thermal equilibrium population. In the following, we present the most recent results related with the question of equilibration of secondaries in heavy ion collisions and discuss its possible relation with deconfinement.

3 Statistical model and particle multiplicity

The basic quantity in the statistical model description of thermal properties of hadronic matter is the partition function $Z(T, V)$. In the Grand Canonical (GC) ensemble,

$$Z^{GC}(T, V, \mu_Q) \equiv \mathrm{Tr}[e^{-\beta(H-\sum_i \mu_{Q_i} Q_i)}], \tag{3}$$

where H is the hamiltonian of the system, Q_i are the conserved charges and μ_{Q_i} is the chemical potentials that guarantees that the charge Q_i is conserved on the average in the whole system. Finally $\beta = 1/T$ is the inverse temperature.

In the strongly interacting medium, one includes the conservation of electric charge, baryon number and strangeness. Thus, the partition function depends in general on five parameters. However, only three are independent, since the isospin asymmetry in the initial state fixes the charge chemical potential and strangeness neutrality conditions eliminate the strange chemical potential. On the level of particle multiplicity ratios derived from the partition function, we are left with only temperature T and baryon chemical potential μ_B as independent parameters.

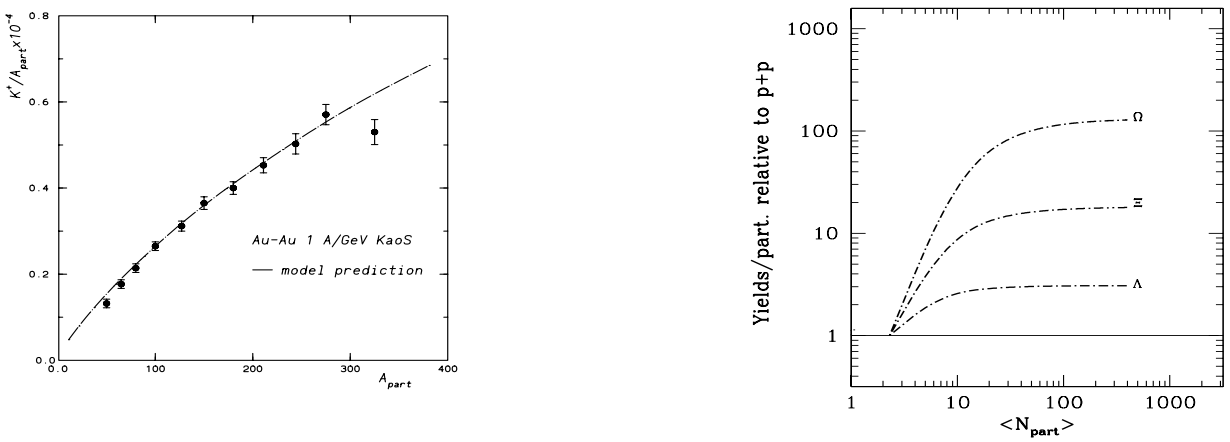

Figure 3: On the left, the ratio of kaon to pion measured in Au–Au collisions at 1 A GeV [44]; the broken line represents the statistical model results [36]. The rights–hand figure shows statistical model predictions for yield/participants in A–A collisions at 40 A GeV normalized to the corresponding value in pp collisions.

The Hamiltonian is usually described by the hadron resonance gas, which contains the contributions from all mesons with masses below 1.6 GeV and baryons with masses below 2 GeV. In this mass range the hadronic spectrum is well established and the decay properties of resonances are known. This mass cut in the contribution to partition function limits, however, the maximal temperature to $T_{\max} < 190$ MeV, up to which the model predictions could be trustworthy. For higher temperatures the contributions of heavier resonances are not negligible.

In the high density regime the repulsive interactions of hadrons should also be included in the partition function. To incorporate the repulsion on short distances between hadrons one usually uses a hard core description by implementing the excluded volume corrections. In the thermodynamically consistent approach [34] these corrections lead to a shift of baryon chemical potential. Finally, the widths of resonances and their decay into lighter particles have to be included in the statistical model when calculating particle multiplicities [18, 36].

The statistical model, described above, was applied to Pb–Pb collisions at top SPS energy [17, 18, 19]. The model was compared with almost all experimental data obtained by NA44, NA49 and WA97 Collaboration. Hadron multiplicities ranging from pion to omega and their ratios were used to verify if there is a set of thermal parameters (T, μ_B) that simultaneously reproduces all measured yields. A detailed analysis has shown [18] that choosing a temperature $T = 168 \pm 4$ MeV and a baryon chemical potential $\mu_B = 266 \pm 8$ MeV, the statistical model with only two parameters can indeed describe seventeen different particle multiplicity ratios within an accuracy of one to two standard deviations. One could thus conclude that, with respect to the statistical operator formulated for equilibrium hadron resonance gas, the experimental data at the SPS are showing a high level of chemical equilibration. The natural question arising here would be to what extent this statistical operator provides a unique description of

the data. This question was addressed in the literature and two distinct models have been examined [7, 37]. In [37] the authors analysed the possible influence of in-medium effects on the chemical equilibrium description of particle yields at the SPS. In [7] the non-equilibrium scenario of explosive hadronization of a QGP fireball was proposed. Both these models and particularly [7] are showing satisfactory agreement with SPS data, however with larger deviations for multistrange particles. In our discussion we concentrate on equilibrium description of particle production since only this approach, as will be demonstrated, provides the systematic agreement with almost all heavy ion data from SIS to RHIC.

The chemical freeze–out temperature, found from a thermal analysis [18, 19] of experimental data in Pb–Pb collisions at the SPS is remarkably consistent, within errors, with the critical temperature $T_c \simeq 173 \pm 8$ MeV obtained from lattice Monte-Carlo simulations of QCD at vanishing baryon density [23]. Thus, the observed hadrons seem to be originating from a deconfined medium and the chemical composition of the system is most likely to be established during hadronization [4, 5, 6]. The observed coincidence of chemical and critical conditions in the QCD medium, if indeed valid, should be seen also in heavy ion collisions at higher collision energies, in particular at RHIC.

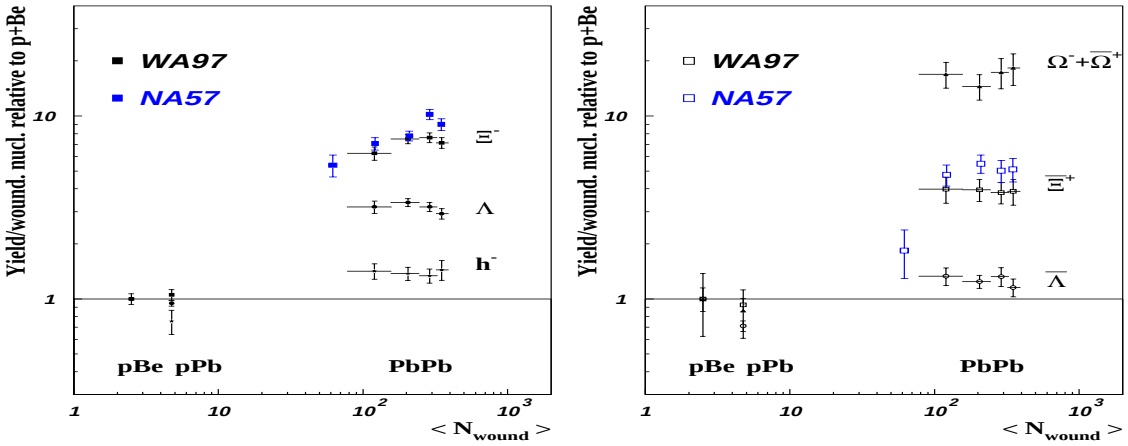

Figure 4: Particle yields per participant in Pb+Pb relative to p+Be and p+Pb collisions centrality dependence. The data are from WA97 [46] and NA57 [49] Collaborations.

The equilibrium statistical model was recently applied to Au–Au collisions at $\sqrt{s} = 130$ GeV at RHIC [35]. The results of the STAR, PHENIX, PHOBOS and BRAHMS Collaboration for different particle multiplicity ratios have been used to test chemical equilibration at RHIC. In Fig. 2 we show the comparison of the thermal model with experimental data. One sees that the overall agreement is very good. Most of the data are reproduced by the model within the experimental errors. The largest deviations are seen in the ratios of $\bar{K}^{*0}/h^-$ and K^{*0}/h^- but they are still on the level of one standard deviation.[2] In Au–Au collisions at $\sqrt{s}$= 130 GeV the chemical freeze–out appears at $T = 175 \pm 7$ MeV and $\mu_B = 51 \pm 6$ MeV. The resulting temperature is only slightly higher than that previously found at the SPS where for Pb-Pb

[2]In the model calculations, the h^- was considered as the total number of negatively charged particles in the thermal fireball

collisions $T = 168 \pm 5$MeV. This relatively moderate increase of temperature could be expected since, in the limit of vanishing baryon density, the temperature should not exceed the critical value required for deconfinement. The substantial decrease of the baryon chemical potential from $\mu_B \simeq 270$ MeV at the SPS to $\mu_B \simeq 50$ MeV at RHIC shows that, at midrapidity, we are dealing with a low net baryon density medium.

The results for particle yields and their ratios at the SPS and RHIC shows the statistical order. Chemical equilibration of secondaries after hadronization is rather excluded by kinetics [15, 39]. Thus, the equilibrium population of hadrons would be most likely to appear since it was pre–established in the QGP phase. In the following we argue, however, that equilibration of secondaries is not a unique signal for deconfinement, as it is also there at lower energies, where the initial conditions exclude QGP formation. To test equilibration in low energy nucleus-nucleus collisions, one needs, however, to change the statistical operator from a GC to a canonical C ensemble with respect to strangeness conservation.

4 Equilibrium limit of rarely produced particles

The conservation of quantum numbers related with U(1) internal symmetry in statistical models can be described in the GC ensemble only if the number of produced particles per event carrying corresponding quantum number is much larger than 1. In the opposite limit of rare particle production [40, 41], U(1) charge conservation must be implemented locally on an event-by-event basis, i.e., a canonical C ensemble of conservation laws must be used. The C ensemble is relevant in the statistical description of particle production in low energy heavy ion [36], or high energy hadron–hadron or e^+e^- reactions [38] as well as in peripheral heavy ion collisions [42].

The exact conservation of quantum numbers, that is the canonical approach, is known to severely reduce the thermal phase–space available for particle production [40]. Consequently, the chemical equilibrium limit of rarely produced particles is changed and it is different from the one obtained in the asymptotic GC limit. In order to illustrate the above change, let us consider the kinetics for the time evolution and equilibration of rarely produced particles by considering a simple example of K^+K^- pair production and equilibration in the environment of thermal pions contained in volume V at temperature T. The production of kaons is due to the binary process $\pi^+\pi^- \to K^+K^-$.

In the standard formulation [43], the rate equation for this binary process is described by the following population equation:

$$\frac{d\langle N_K\rangle}{d\tau} = \frac{G}{V}\langle N_{\pi^+}\rangle\langle N_{\pi^-}\rangle - \frac{L}{V}\langle N_{K^+}\rangle\langle N_{K^-}\rangle, \tag{4}$$

where $G \equiv \langle \sigma_G v\rangle$ and $L \equiv \langle \sigma_L v\rangle$ give the momentum-averaged cross sections for the gain $\pi^+\pi^- \to K^+K^-$ and the loss $K^+K^- \to \pi^+\pi^-$ process, respectively, and $\langle N_K\rangle$ represents the total number of produced kaons.

In the above equation it is explicitly assumed that K^+ and K^- are uncorrelated. To include possible correlations between the production of K^+ and K^- [41], let us define $P_{i,j}$ as the probability to find i number of K^+ and j number of K^- in an event. We also denote by

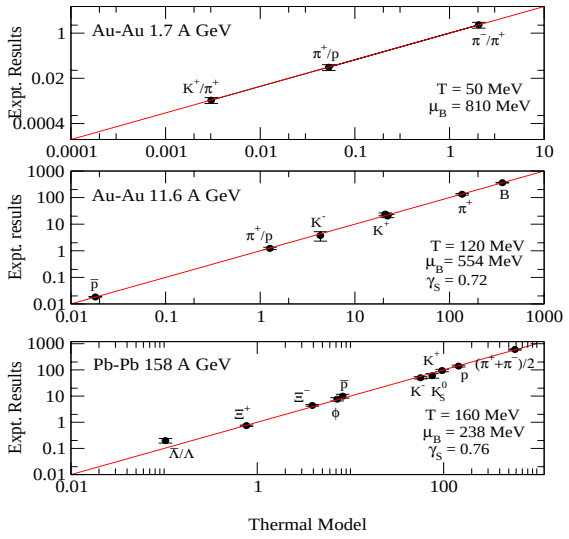

FIGURE 4b.
Comparisons of the experimental data (vertical scale) for different particle multiplicity ratios obtained in Au–Au and Pb–Pb collisions at SIS, AGS and SPS with the statistical model predictions [19].

P_i the probability to find i number of K in an event. The average number of K per event is defined as: $\langle N_K \rangle = \sum_{i=0}^{\infty} i P_i$.

We can now write the following general rate equation for the average kaon multiplicities:

$$\frac{d\langle N_K \rangle}{d\tau} = \frac{G}{V}\langle N_{\pi^+} \rangle \langle N_{\pi^-} \rangle - \frac{L}{V}\sum_{i,j} ij P_{i,j}. \tag{5}$$

Owing to the local conservation of quantum numbers, we have:

$$\begin{aligned} P_{i,j} &= P_i\ \delta_{ij}, \\ \sum_{i,j} ij P_{i,j} &= \sum_i i^2 P_i \equiv \langle N^2 \rangle = \langle N \rangle^2 + \langle \delta N^2 \rangle, \end{aligned} \tag{6}$$

where $\langle \delta N^2 \rangle$ represents the event-by-event fluctuation of the number of K^+K^- pairs. Note that we always consider abundant π^+ and π^- so that we can neglect the number fluctuation of these particles and the change of their multiplicities due to the considered processes.

Following Eqs. (5) and (6) the general rate equation for the average number of K^+K^- pairs can be written as:

$$\frac{d\langle N_K \rangle}{d\tau} = \frac{G}{V}\langle N_{\pi^+} \rangle \langle N_{\pi^-} \rangle - \frac{L}{V}\langle N_K^2 \rangle. \tag{7}$$

For abundant production of K^+K^- pairs where $\langle N_K \rangle \gg 1$, $\langle N_K^2 \rangle \approx \langle N_K \rangle^2$, and Eq. (7) obviously reduces to the standard form:

$$\frac{d\langle N_K \rangle}{d\tau} \approx \frac{G}{V}\langle N_{\pi^+} \rangle \langle N_{\pi^-} \rangle - \frac{L}{V}\langle N_{K^+} \rangle \langle N_{K^-} \rangle. \tag{8}$$

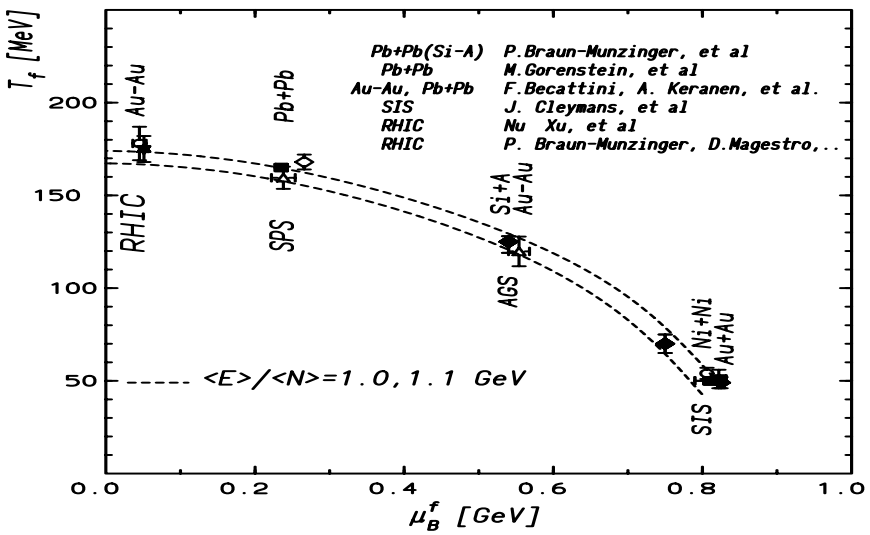

Figure 5: Compilation of chemical freeze–out parameters from SIS to RHIC. The broken line represents a phenomenological condition of chemical freeze–out of fixed energy/particle $\simeq$ 1 GeV [17].

However, for rare production of K^+K^- pairs where $\langle N_K\rangle \ll 1$, the rate equations (4) and (8) are no longer valid. We have instead $\langle N_K^2\rangle \approx \langle N_K\rangle$, which reduces Eq. (7) to the form [41]:

$$\frac{d\langle N_K\rangle}{d\tau} \approx \frac{G}{V}\langle N_{\pi^+}\rangle\langle N_{\pi^-}\rangle - \frac{L}{V}\langle N_K\rangle. \tag{9}$$

Thus, the limit where $\langle N_K\rangle \ll 1$, the absorption term depends on the pair number only linearly, instead of quadratically for the limit of $\langle N_K\rangle \gg 1$. It is thus clear, that the time evolutions and equilibrium values for kaon multiplicities are obviously different in the above limiting situations.

In the limit of large $\langle N_K\rangle$ the equilibrium value for the number of K^+K^- pairs, which coincides with the multiplicity of K^+ and K^-, is obtained from Eq. (8) as,

$$\langle N_K\rangle_{\rm eq}^{\rm GC} = \frac{V}{2\pi^2} m_K^2 T K_2(M_K/T), \tag{10}$$

it is thus described by the GC result with vanishing chemical potential, in our example, because of the strangeness neutrality condition.

In the opposite limit, where $\langle N_K\rangle \ll 1$, the time evolution of pion multiplicity is described by Eq. (9), which has the following equilibrium solution:

$$\langle N_K\rangle_{\rm eq}^{\rm C} = \left[\frac{V}{2\pi^2} M_{K^+}^2 T K_2(M_{K^+}/T)\right]\left[\frac{V}{2\pi^2} M_{K^-}^2 T K_2(M_{K^-}/T)\right]. \tag{11}$$

The above equation demonstrates the locality of strangeness conservation. With each K^+ the K^- is produced in the same event in order to conserve strangeness exactly and locally.

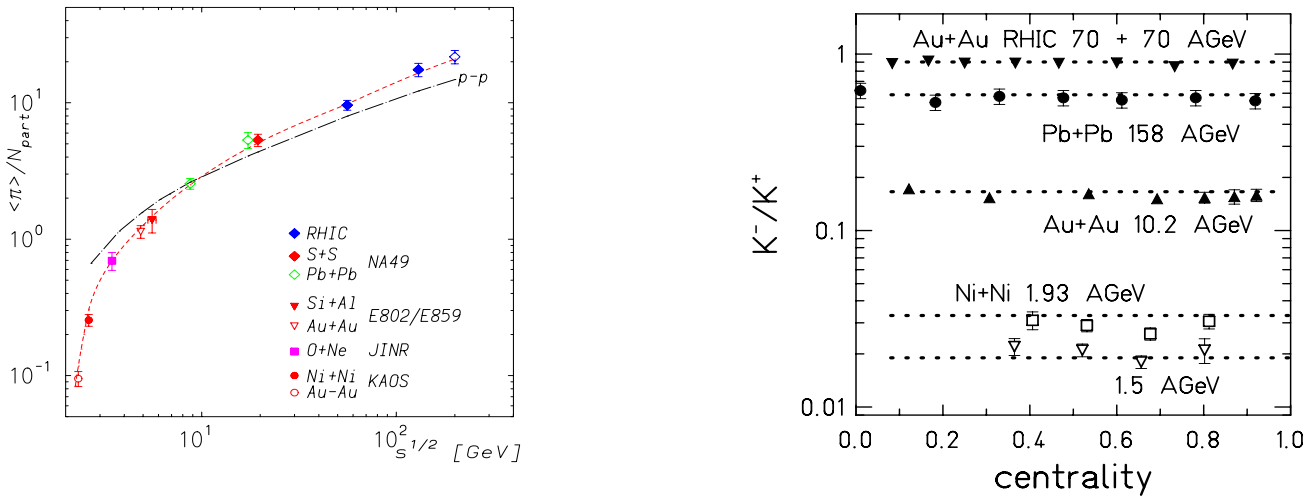

Figure 6: The left-hand figure shows the total number of pions per participant ($\langle\pi\rangle/N_{\rm part}$), 4π data in A–A and p–p collisions versus energy. Data at lower energies in A–A as well as in p–p collisions are from [65]. The RHIC results are from [66]. The short-dashed and dashed lines represent the fit to the data. The right-hand figure shows the centrality dependence of the K^+/K^- ratio. Data are from the STAR, NA49, E866, and KaoS Collaborations. The broken lines are statistical model results.

Comparing Eqs. (10) and (11), we first find that, for $\langle N_K\rangle \sim 1$, the equilibrium value is far smaller than what is expected in the opposite limit. We also note that the volume dependence differs in the two cases . The *particle density* in the $\langle N_K\rangle \gg 1$ limit is independent from V whereas in the opposite limit the density scales linearly with V.[3]

The results of Eqs. (10) and (11) correspond to two limiting cases of asymptotically large and small kaon multiplicity in heavy ion events. In order to find the equilibrium solution valid for any arbitrary number of kaons per events one needs to formulate a kinetic equation for the probability instead of the multiplicity of produced particles [41].

Let $P_n(t)$ $(0 \le n \le \infty)$ be the probability function for the production of n, K^+K^- pairs. The probability P_n tends to increase in time owing to the transition from $n-1$ and $n+1$ states to n. It also tends to decrease since the state n makes a transition to $n+1$ and $n-1$. With the transition probability per unit time from $n \to n+1$ given by $GN_{\pi^+}N_{\pi^-}V^{-1}$ and from $n-1 \to n$ described as LV^{-1}, one can formulate the general iterative master equation for the probability function as [41]:

$$\begin{aligned} \frac{dP_n}{d\tau} &= \frac{G}{V}N_{\pi^+}N_{\pi^-}(P_{n-1}-P_n) \\ &- \frac{L}{V}\left[n^2P_n-(n+1)^2P_{n+1}\right]. \end{aligned} \tag{12}$$

The above equation is equivalent to the general rate equation described by Eq. (7). However, contrary to Eq. (7) it can be solved for the equilibrium limit corresponding to an arbitrary

[3]In the application of the statistical model to particle production in heavy ion collisions, the volume of the fireball scales with the number of participating nucleons $N_{\rm part}$. Thus, in terms of the canonical model, depending on the abundances of produced U(1) charged particles, one obviously expects different centrality dependences.

number of produced kaons. Indeed, converting first the above equations for P_n's into a partial differential equation for the generating function $g(x,\tau) = \sum_{n=0}^{\infty} x^n P_n(\tau)$ one obtains

$$\frac{\partial g(x,\tau)}{\partial \tau} = \frac{L}{V}(1-x)\left(xg'' + g' - \epsilon g\right), \tag{13}$$

where $g' \equiv \partial g/\partial x$ and $\sqrt{\epsilon} \equiv \langle N_K \rangle_{\rm eq}^{GC}$ given by Eq. (10). The equilibrium solution for $g_{\rm eq}(x)$ is obtained as

$$g_{\rm eq}(x) = \frac{1}{I_0(2\sqrt{\epsilon})} I_0(2\sqrt{\epsilon x}), \tag{14}$$

where the normalization is fixed by $g(1) = \sum P_n = 1$.

The equilibrium value for the probability function P_n is expressed by

$$P_{n,\rm eq} = \frac{\epsilon^n}{I_0(2\sqrt{\epsilon})(n!)^2}, \tag{15}$$

which converts to a Poisson distribution only in the limit of the large argument of the Bessel function.

The result for the average number of kaon pairs K^+K^- in equilibrium is obtained from $g'(1)$ and reads:

$$\langle N_K \rangle_{\rm eq}^{C} = \frac{V}{2\pi^2} m_K^2 T K_2(M_K/T) \times \frac{I_1[2\frac{V}{2\pi^2} m_K^2 T K_2(M_K/T)]}{I_0[2\frac{V}{2\pi^2} m_K^2 T K_2(M_K/T)]}. \tag{16}$$

The above equation is a general equilibrium solution, which is valid for an arbitrary value of $\langle N_K \rangle$ and obviously reproduces the asymptotic results described by Eqs. (10) and (11). This can be seen in the most transparent way when comparing two limiting situations: the large–and–small x (where x is the argument of the Bessel function) limit of the above equation.

The equilibrium density corresponding to a large N_K limit and described by Eq. (10) is a standard result for the particle density that can be obtained from the GC partition function introduced in Eq. (3). The general results described by Eq. (16) obviously require a different definition of the partition function, which takes into account the exact conservation of quantum numbers. This is the canonical partition function with respect to the charge conservation. In the C approach there is no more chemical potential under the trace as in Eq. (3) but, instead, the partition function is calculated by summing only those states that are carrying exactly the quantum number Q, that is

$$Z_Q^C(T,V) \equiv {\rm Tr}_Q[e^{-\beta H}]. \tag{17}$$

Following Eq. (6) it is clear that C and GC limits are essentially determined by the size of $\langle \delta N^2 \rangle$, the event-by-event fluctuations of the number of particles carrying U(1) charge. The grand canonical results correspond to small fluctuations, i.e. $\langle \delta N^2 \rangle / \langle N \rangle^2 \ll 1$, while the canonical description is necessary in the opposite limit.

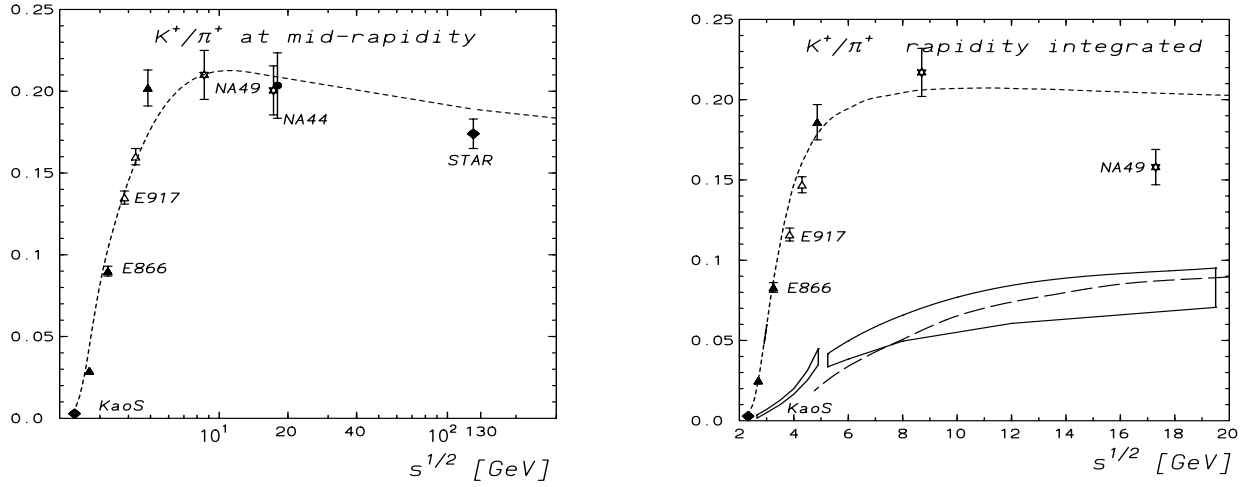

Figure 7: Ratio of kaon to pion measured in heavy ion collision at different collisions energies. The left-hand figure corresponds to midrapidity data, whereas the right one represents the ratios, of fully integrated results. Data at SIS, AGS, SPS and RHIC are taken from [50, 51]. The short-dashed line describes the results calculated following the freeze–out curve shown in Fig. 5. The parameterization of the p–p data from [53] is indicated by the fulls-line.

The major difference between the canonical and the grand canonical treatment of the conservation laws appears through a different volume dependence of particle densities as well as a strong suppression of the thermal particle phase space in the former. The relevant parameter to measure the suppression of particle multiplicities from their grand canonical result is seen, in Eq. (16), to be determined by the ratio of the Bessel functions $I_1(x)/I_0(x)$. For multistrange particles this suppression factor has a more complicated structure [42, 45].

In nucleus–nucleus collisions the absolute values of baryon number, electric charge and strangeness are fixed by the initial conditions. Modelling particle production in statistical thermodynamics would in general require the canonical formulation of all these quantum numbers. A detailed analysis [40, 47], however, has shown that in heavy ion collisions only strangeness should be treated exactly, whereas the conservation of baryon and electric charges can be described by the appropriate chemical potentials in the grand canonical ensemble.

In heavy ion collisions the number of produced strange particles depends on the collision energy and centrality of these collisions. At low collision energies, at SIS/GSI for example, the average number of strange particles produced in an event is much smaller than 1. Thus, here we are in the asymptotic regime of canonical ensemble. Figure 3a shows the experimental data on K^+ yield per participant $A_{\rm part}$ as a function of $A_{\rm part}$ measured in Au–Au collisions at $E_{\rm lab} \sim 1$ A/GeV [44]. The data are compared with the results of the canonical statistical model shown by the dashed–line. The thermal parameters, the temperature and the baryon chemical potential were chosen in such a way as to reproduce measured particle multiplicity ratios of strangeness neutral particles [36]. The volume parameter in the statistical operator is assumed to scale with the number of participants. The results in Fig. 3a clearly indicate that both the

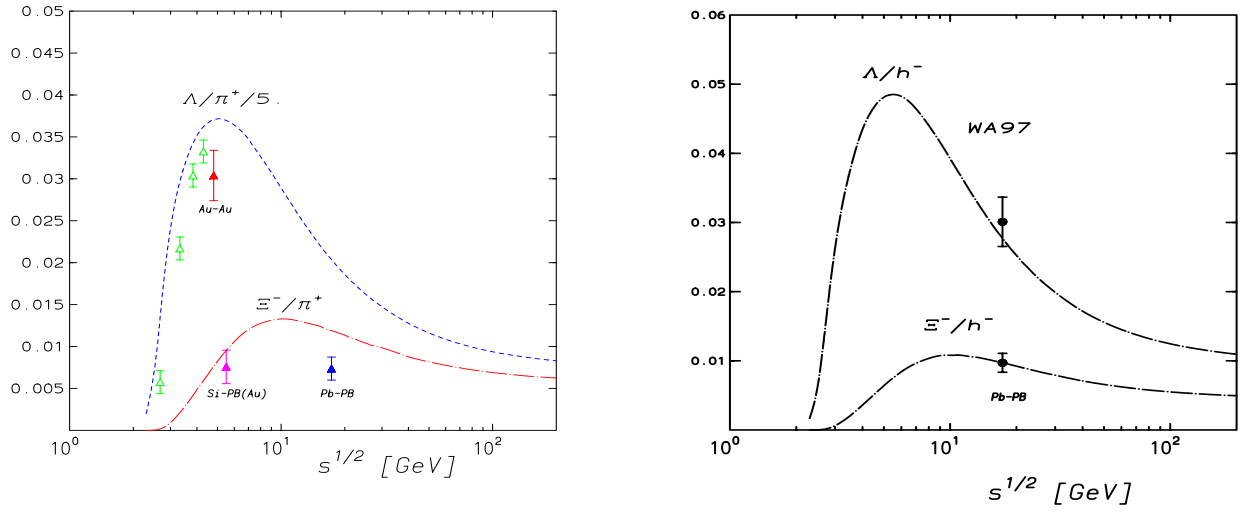

Figure 8: Particle ratios in A–A versus energy. Data at the SPS are fully integrated NA49 results (left-hand figure). The right-hand figure shows WA97 data at midrapidity. The corresponding ratio at the top AGS was obtained from E810 results on Ξ^- measured in Si–Pb collisions in the rapidity interval $1.4 < y < 2.9$ [55], normalized to the full phase space values of π^+ and K^- yield obtained in Si–Au collisions by E802 [56]. The lines represent statistical model results along the unified freeze–out curve from Fig. 5.

magnitude of the yield and the strong, almost quadratic, dependence of the kaon yield on the number of participants is well reproduced by the canonical model.

The importance of the canonical treatment of strangeness conservation has been shown also at higher collision energies, e.g., at the SPS or even RHIC, when considering the centrality dependence of multistrange baryons [42]. In very peripheral collisions the yield of strange particles is so small that the canonical description should be applied there as well. The canonical suppression of the thermal particle phase–space was found to increase with the strangeness content of the particle.

Figure 3b shows the multiplicity/participant of Ω, Ξ, and Λ relative to its value in p–p or p–A collisions [42]. Thermal parameters $T = 145$ MeV and $\mu_B = 370$ MeV were used here and assumed to be centrality–independent. These values are expected in Pb–Pb collisions at 40 AGeV. Figure 3b indicates that the statistical model in the C ensemble reproduces the basic features of the WA97 data [46] shown in Fig. (4): the enhancement pattern and enhancement saturation for large $A_{\rm part}$. Figure 4 also demonstrates a different $A_{\rm part}$ dependence of strange and multistrange baryons as well as a much larger enhancement at 40 A GeV than seen in WA97 data at top SPS. The basic predictions of the canonical statistical model is that strangeness enhancement from p–p to A–A collisions should increase with decreasing energy. This result is in contrast with UrQMD finding [48] and with previous qualitative predictions that the strangeness enhancement is being entirely due to quark–gluon plasma formation [15].

The quantitative comparison of the canonical model with the experimental data of WA97

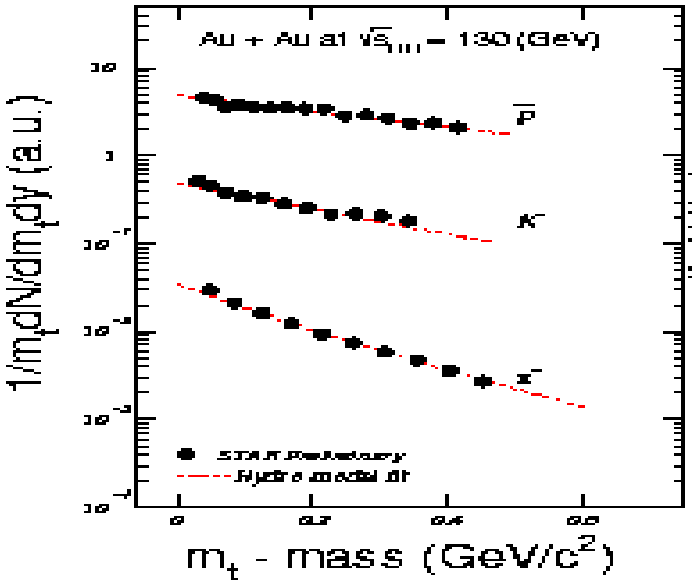

Figure 9: Transverse momentum distribution of pion, proton and kaon obtained by STAR at $\sqrt{s} =$ 130 GeV [57]
.

has been discussed in [42]. The most recent results of NA57 [49], showing an abrupt change of the enhancement for $\bar{\Xi}$ as seen in Fig. 4 are, however, very unlikely to be reproducible in terms of the canonical approach.

5 Particle yields and energy dependence

In the last section arguments were presented in favour of the need for that a more general treatment of U(1) charge conservation, based on the canonical ensemble, if one compares the statistical model with experimental data for particle yields in central A–A collisions at SIS energies or even in peripheral collisions at the SPS and RHIC. A detailed analysis of the experimental data in heavy ion collisions from SIS through AGS has shown that the canonical statistical model reproduces most of the measured hadron yields. Figure 4b shows an example of the recent systematic study of the comparison of the statistical model with a fully integrated particle multiplicities data in central Au–Au and Pb–Pb collisions at beam momenta of 1.7 A/GeV, 11.6 A/GeV (Au-AU) and 158 A/GeV (Pb-PB) [19]. The overall agreement is seen to be very good.

Figure 5 shows the compilation of chemical freeze–out parameters required to reproduce measured particle yields at SIS, AGS, SPS and RHIC energies. The GSI/SIS results have the lowest freeze–out temperature and the highest baryon chemical potential. As the beam energy is increased a clear shift towards higher T and lower μ_B occurs. There is a common feature to all these points, namely that the average energy per hadron is approximately 1 GeV.

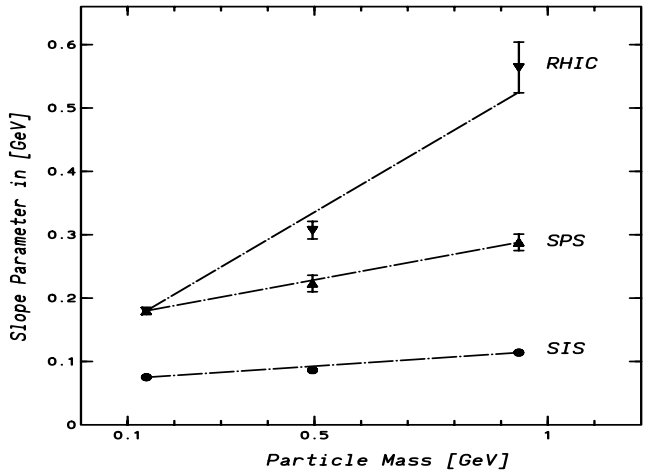

Figure 10: Slope parameters versus particle mass at SIS [36], top SPS [59] and RHIC [57].

Chemical freeze–out in A–A collisions is thus reached *when the energy per particle drops below 1 GeV* at all collision energies [17]. The above phenomenological freeze–out condition provides the relation between temperature and chemical potential at all collision energies. This together with the measured ratio of pion/participant shown in Fig. 6a establishes the energy dependence of the two independent thermal parameters, the temperature and baryon chemical potential. Consequently the definite predictions of particle excitation functions can be given in terms of this model. Figures 6-8 are showing statistical model results for different particle multiplicity ratios along the unified freeze–out curve in comparison with experimental data.

The statistical model predicts that the particle/antiparticle ratio should be independent from centrality for all collision energies. Dynamically this is a rather surprising result as particles and their anti–particle are generally produced and absorbed in surrounding nuclear medium in different ways. Figure 7b represents the energy and centrality dependence of the K^+/K^- ratio from SIS to RHIC. The statistical model predictions are seen in Fig. 6b to agree remarkably well with the data. The measured K^+/π^+ ratio [50] is a very abruptly increasing function of collision energy between SIS up to top AGS. At higher energies it reaches a broad maximum between 20 AGeV - 40 AGeV and gradually decreases up to RHIC energy [51]. In the microscopic transport models [52] the increase of the kaon yield with collision energy is qualitatively expected as being due to a change in the production mechanism from associated to direct kaon emission. However, the hadronic cascade transport models do not, until now, provide quantitative explanation of the experimental data in the whole energy range. The statistical model in the C formulation, on the other hand, provides an excellent description of K/π *midrapidity* data in the whole energy range from SIS up to RHIC, as seen in Fig. 7a. The abrupt increase from SIS to AGS and broad maximum of this ratio are a consequence of the specific dependence of thermal parameters on collision energy and canonical strangeness suppression at SIS. In general, however, results with the statistical model should be compared with 4π-integrated yields, since strangeness does not have to be conserved in a limited portion

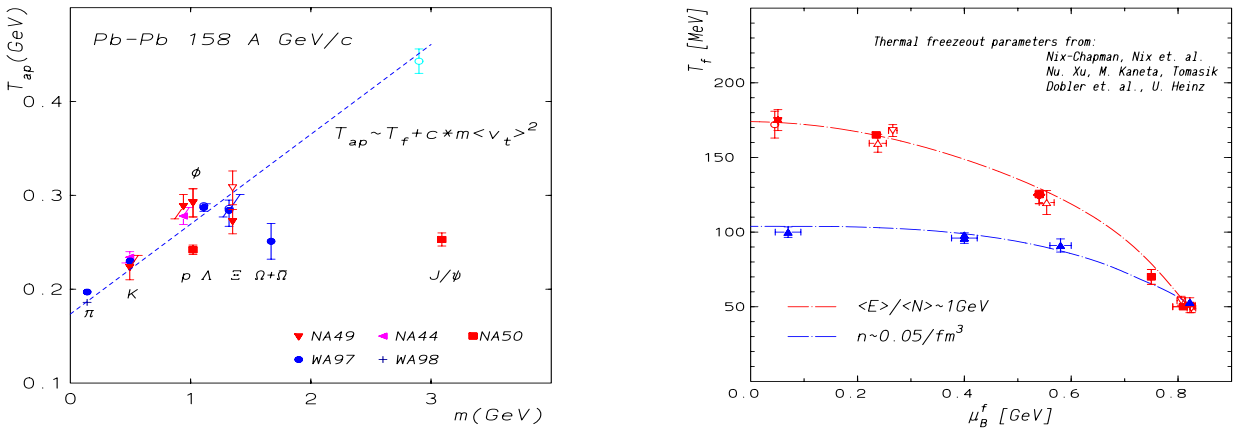

Figure 11: Left: slope parameters at the SPS for different particle species. For the compilation of data, see for instance [59, 58]. Right: Chemical and thermal freeze–out curve from SIS to RHIC. Thermal freeze–out points are from [20, 60].

of phase space. A drop in the K^+/π^+ ratio for 4π yields has been reported from preliminary results of the NA49 Collaboration at 158 AGeV [50] (see Fig. 7b). This decrease is, however, not reproduced by the present statistical model without further modifications, e.g. by introducing an additional parameter $\gamma_s \sim 0.7$ [19] or by formulating a statistical model *of the early stage* [54].

The appearance of the maximum in the relative strange/non-strange particle multiplicity ratios already seen in K^+/π^+ is even more pronounced for strange baryons/meson. Figure 8 shows the energy dependence of Λ/π^+ and Ξ^-/π^+. There is a very clear pronounced maximum especially in the Λ/π^+. This maximum is related with a rather strong decrease of chemical potential coupled with an only moderate increase in associated temperature with increasing energy. The relative enhancement of Λ is stronger than that of Ξ^-. There is also a shift of the maximum to higher energies for particles with increasing strangeness quantum number. This is because the enhanced strangeness content of hadron suppresses the dependence of the corresponding ratio on μ_B. The actual experimental data both for Λ/π^+ and Ξ^-/π^+ ratios shown in Fig. 8 are following the predictions of the statistical model. However, as in the case of kaons, midrapidity results (see Fig. 8b are better reproduced by the model than 4π data (see Fig. 8a).

6 Particle spectra and energy dependence

The agreement of the equilibrium statistical model with experimental data suggests that the collision fireball is of thermal nature. However, this fireball is not a static object. At chemical freeze–out the density inside a fireball is still so high that its constituents undergo strong rescatterings. These rescatterings result in thermodynamic pressure, which causes collective ex-

pansion of the medium. Consequently the particle transverse momentum distribution is showing a slope, which is increasing with the rest mass of the particle. This is a typical behaviour expected from a system which undergoes transverse collective expansion. As an illustration, Fig. 9 shows the recent RHIC results of the STAR Collaboration for the p_t distribution of pion, kaon and proton [57].

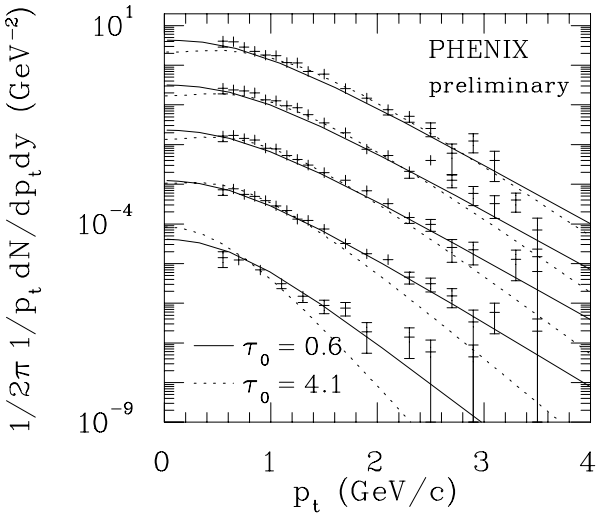

Figure 12: Transverse momentum distribution of antiprotons obtained at RHIC by the PHENIX Collaboration for different centrality [64].

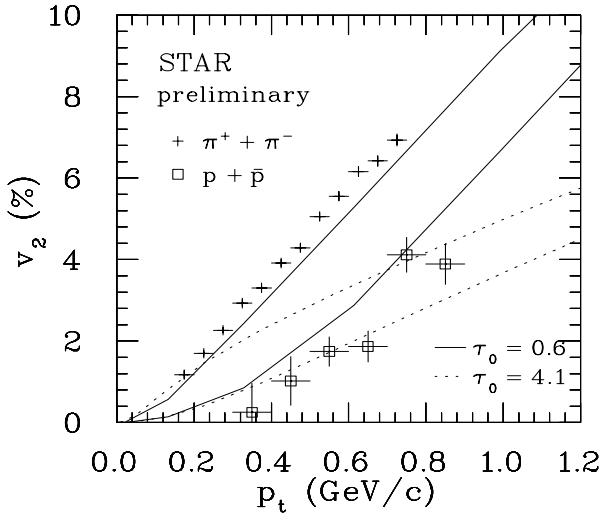

Figure 13: Elliptic flow parameter v_2 of pions and protons+antiprotons in minimum bias collisions at RHIC [64]. Lines represent hydrodynamical model calculations from [62].

The collective transverse flow is, however, not only seen in high energy data. In Fig. 10 the dependence of the slope parameters of pion, kaon and proton is seen to be an increasing function of particle mass from SIS through SPS up to RHIC energy. The measured particle spectra at all energies seem to be affected by both thermal and transverse collective motion. If all particles kinetically decoupled approximately at the same time, then hadronic m_t spectra could be characterized by only two parameters: average thermal freeze–out temperature $\langle T_f \rangle$ and average flow velocity $\langle v_t \rangle$ [11]. A detailed analysis has shown that this works indeed within currently available data and at all energies with the exception of Ω and J/ψ at the SPS which are showing slopes lower than expected from flow systematics (see Fig. 11a. These heavy particles are most likely decoupled from the system already at chemical freeze–out because of their very low rescattering cross section with surrounding hadrons. The compilation of the thermal freeze–out parameters extracted from a detailed analysis of experimental data at SIS [36], the AGS [20], the SPS [20] and most recently at RHIC [60] is shown in Fig. 11b. At SIS, the thermal and chemical freeze–out coincide. At higher energies the thermal freeze–out follows the chemical one. The freeze–out temperature is remarkably consistent at AGS, SPS and RHIC between 100–120 MeV. Hydrodynamic evolution models [61, 62, 63], however, reported recently that at RHIC, $\langle T_f \rangle \simeq 128 - 140$ could thus be slightly higher than at the SPS. Particle p_t spectra at RHIC are very well described within the concept of thermalization

and hydrodynamical evolution. Figure 12 shows an excellent agreement of the hydrodynamical model [62] with preliminary PHENIX data [64] for proton p_t spectra measured at different centrality.

The transverse flow also affects other observables, which are sensitive probes of collective motion and equilibration in heavy ion collisions. One of these observables is the elliptic flow. This is particularly sensitive to the initial conditions and initial rescattering between constituents. It describes the azimuthal momentum-space anisotropy of particle emission in non-central heavy ion collisions. This emission is measured in the plane transverse to the beam direction. The parameter that characterizes the elliptic flow is the second coefficient v_2 of an azimuthal Fourier decomposition of the particle p_t spectra. Figure 13 shows that minimum bias data at RHIC for v_2 are very well described by a hydrodynamical model [62, 63] up to $p_t \simeq 2$ GeV. Deviations are seen both for higher transverse momentum and for detailed centrality analysis of experimental data [62, 63]. An excellent agreement of RHIC experimental data both for particle yields and soft p_t spectra indicates an early thermalization of the QCD medium already on the partonic level and its further hydrodynamical evolution.

7 Summary and conclusions

We have reviewed some properties of the experimental data on particle yields and their spectra measured in A–A collisions from SIS up to RHIC energy. We have shown that at all energies particles seem to be produced according to the principle of maximal entropy, showing the statistical order of the multiplicities. Particle spectra, on the other hand, can be satisfactorily described by introducing in addition to thermal also transverse collective motion. A large degree of thermalization and collectivity in experimental data is particularly evident at RHIC and the SPS. Here chemical freeze–out conditions are remarkably consistent with those expected for deconfinement, and particle spectra are well described by transverse collective flow. Until now, however, there is no rigorous theoretical understanding of the thermal nature of particle production in heavy ion collisions. At RHIC and the SPS the appearance of the QGP in the initial state could be a driving force towards equilibration. At low collision energies the necessary conditions for deconfinement are not satisfied; thermalization is thus most likely to take place through production and rescattering of hadronic constituents.

8 Acknowledgements

We acknowledge stimulating discussions with P. Braun-Munzinger, J. Cleymans, V. Koch, H. Oeschler, H. Satz, R. Stock and A. Tounsi. The partial support of the Polish Committee for Scientific Research (KBN-2P03B 03018) is also acknowledged.

References

[1] For a recent review, see e.g. S.A. Bass, M. Gyulassy, H. Stocker, and W. Greiner, J. Phys. G25 R1 (1999);

H. Satz, Rep. Prog. Phys. 63 (2000) 1511.

[2] E. V. Shuryak, Phys. Rep. 115 (1984) 151; J. Cleymans, R.V. Gavai and E. Suhonen, Phys. Rept. 130 (1986) 217.

[3] T. Hatsuda, these Proceedings.

[4] R. Stock, Phys. Lett. 456 (1999) 277; Prog. Part. Nucl. Phys. 42 (1999) 295.

[5] J. Stachel, Nucl. Phys. A654 (1999) 119c.

[6] U. Heinz, Nucl. Phys. A685 (2001) 414 and A661 (1999) 349.

[7] J. Letessier, and J. Rafelski, Int. J. Mod. Phys. E **9**, 107 (2000).

[8] J. Alam, et al., hep-th/010802; Ann. Phys. 286 (2001) 159

[9] D. K. Srivastava, Eur. Phys. J. 10 (1999) 487.

[10] R. Rapp, Phys. Rev. C63 (2001) 054907.

[11] U. A. Wiedemann and U. Heinz, Phys. Rep. 319 (1999) 145, and references therein.

[12] For a recent review, see e.g., G. E. Brown and M. Rho, hep-ph/0103102.

[13] T. Matsui and H. Satz, Phys. Lett. B178 (1986) 416.

[14] H. W. Barz, H. Schulz, B. L. Friman and J. Knol, Phys. Lett. B254 (1991) 315, Nucl. Phys. A545 (1992) 259.

[15] P. Koch, B. Müller, and J. Rafelski, Phys. Rep. 142 (1986) 167. J. Rafelski Phys. Lett. B262 (1991) 333.

[16] P. Braun-Munzinger, J. Stachel, J. P. Wessels and N. Xu, Phys. Lett. B344 (1995) 43 and B365 (1996) 1

P. Braun-Munzinger and J. Stachel, Nucl. Phys. A606 (1996) 320.

[17] J. Cleymans and K. Redlich, Phys. Rev. Lett. 81 (1998) 5284 and references therein.

[18] P. Braun-Munzinger, I. Heppe and J. Stachel, Phys. Lett. B465 (1999) 15.

[19] F. Becattini, J. Cleymans, A. Keranen, E. Suhonen and K. Redlich, Phys. Rev. C64 (2001) 024901.

[20] B. Tomasik, U. A. Wiedemann and U. Heinz, Nucl. Phys. A663 (2000) 753; R. Nix, Phys. Rev. C58 (1998) 2303.

[21] J. Sollfrank, et al., Phys. Rev. C55 (1997) 392.

[22] P. Huovinen, et al., Phys. Lett. B503 (2001) 58, and references therein.

[23] F. Karsch, E. Laermann, and A. Peikert, Nucl. Phys. B605 (2001)579.

[24] J. P. Blaizot, E. Iancu, and A. Rebhan, Phys. Rev. D63 (2001) 065003.

[25] R. Pisarski, Phys. Rev. D62 (2000) 111501.

[26] J. D. Bjorken, Phys. Rev. D27 (1983) 140.

[27] M. Agarwal, et al. (WA98 Coll.), Eur. Phys. J. C18 (2001) 651.

[28] L. V. Gribov, et al., Phys. Rep. 100 (1983) 1; A.H. Mueller and J. Qiu, Nucl. Phys. B268 (1986) 427.

[29] K. J. Eskola, K. Kajantie, P. Ruuskanen and K. Tuominen, Nucl. Phys. B570 (2000) 379.

[30] L. McLerran, and R. Venugopalan, Phys. Rev. D49 (1994) 2233 and D49 (1994) 3352; D50 (1994) 2225.

[31] D. Kharzeev and M. Nardi, Phys. Lett. B507 (2001) 121.

[32] R. Baier, A.H. Mueller, D. Schiff, and D.T. Son, Phys. Lett. B502 (2001) 51.

[33] K. Geiger and D. K. Srivastava, Nucl. Phys A661 (1999) 592, nucl-th/9808042;

[34] D. Rischke, M. I. Gorenstein, H. Stocker and W. Greiner, Z. Phys. C51 (1990) 485; G. Yen, et al., Phys. Rev. C51 (1997) 2210.

[35] P. Braun-Munzinger, D. Magestro, K. Redlich, and J. Stachel, Phys. Lett. B518 (2001) 41.

[36] J. Cleymans and K. Redlich, Phys. Rev. C60 (1999) 054908; J. Cleymans, H. Oeschler and K. Redlich, Phys. Rev. C59 (1999) 1663; Phys. Lett. B485 (2001) 27.

[37] D. Zschiesche et al., Nucl. Phys. A681 (2001) 34.

[38] F. Becattini, Z. Phys. C69 (1996) 485; F. Becattini and U. Heinz, Z. Phys. C76 (1997) 269.

[39] R. Rapp and E. Shuryak, Phys. Rev. Lett. 86 (2001) 2980; C. Greiner and S. Leupold, J. Phys. G27 (2001) L95.

[40] R. Hagedorn, Thermodynamics of stron interactions, CERN Report 71-12 (1971); E.V. Shuryak, Phys. Lett. B42 (1972) 357; K. Redlich and L. Turko, Z. Phys. B97 (1980) 279; R. Hagedorn and K. Redlich, Z. Phys. A27 (1985) 541.

[41] C.M. Ko, V. Koch, Z. Lin, K. Redlich, M. Stepanov and X.N. Wang, nucl-th/0010004, Phys. Rev. Lett. 86 (2001) 5438.

[42] J. S. Hamieh, K. Redlich and A. Tounsi, Phys. Lett. B486 (2000) 61.

[43] T. Matsui, B. Svetitsky and L.D. McLerran, Phys. Rev. D34 (1986) 783.

[44] A. Wagner et al. (KaoS Coll.), Phys. Lett. B420 (1998) 20, C. Muntz et al. (KaoS Coll.) Z. Phys. C357 39.

[45] P. Braun-Munzinger, J. Cleymans, H. Oeschler and K. Redlich, nucl-ph/0106066, Nucl. Phys. A in print.

[46] E. Andersen, et al. (WA97 Coll.), Phys. Lett. B449 (1999) 401.

[47] M. Gazdzicki and M. Gorenstein, Phys. Lett. B483 (2000) 60.

[48] M. Bleicher, W. Greiner, H. Stöcker, and N. Xu, Phys. Rev. C62 (2000) 061901.

[49] N. Carrer (NA57 Coll.), in Proceedings of QM2001.

[50] Ch. Blume (NA49 Coll.), in Proceedings of QM2001.

[51] J. Harris (STAR Coll.), in Proceedings of QM2001.

[52] W. Cassing, Nucl. Phys. A661 (1999) 468c.

[53] C. A. Ogilvie, nucl-ex/010410, J. C. Dunlop and C. A. Ogilvie, Phys. Rev. C61 (2000) 031901.

[54] M. Gazdzicki, et al., Z. Phys. C65 (1995) 215, Acta Phys. Pol. B30 (1999) 2705.

[55] S. E. Eiseman et al. (E810 Coll.), Phys. Lett. B297 (1992) 44 and B325 (1994) 322.

[56] T. Abbott et al., E802 Coll., Phys. Rev. C60 (1999) 044904; Y. Akiba et al. (E802 Coll.), Nucl. Phys. A590 (1995) 179c.

[57] Nu Xu, nucl-ex/0104021, in Proceedings of QM2001.

[58] K. Redlich, hep-ph/0105104.

[59] H. van Hecke, H. Sorge and N. Xu, Nucl. Phys. A661 (1999) 493c.

[60] J. Burward-Hoy (PHENIX Coll.), presented at *Workshop on Thermalization in Heavy Ion Collisions*, BNL, July 2001.

[61] U. Heinz, hep-ph/0109006.

[62] P. Huovinen, hep-th/0108033 and these Proceedings.

[63] D. Teaney, J. Lauret and E. Shuryak, Phys. Rev. Lett 86 (2001) 4783; nucl-th/0104041.

[64] J. Velkovska (PHENIX Coll.), nucl-ex/0105012; C. Adler et al. (STAR Coll.), nucl-ex/0107003.

[65] M. Gazdzicki, and D. Roehrich, Z. Phys. C66 (1995) 77.

[66] The 4π results at $\sqrt{s} = 56$ GeV are estimated from PHOBOS mid-rapidity data from [68] scale by the same factor as required in p–p collisions when going from midrapidity to full phase space. The results at $\sqrt{s} = 130$ GeV are from [67]. The 4π results at $\sqrt{s} = 200$ GeV were estimated by multiplying the $\sqrt{s} = 130$ GeV result by the same factor (modulo increase in rapidity interval) as recently measured by PHOBOS at midrapidity [68].

[67] I.G. Bearden, et. al., nucl-ex/0108016.

[68] B.B. Back, et. al., nucl-ex/0105001; Phys. Rev. Lett. 85 (2000) 3100; nucl-ex/0108009.